Differential expression of endothelial nutrient transporters (MCT1 and GLUT1) in the developing eyes of mice

Ayuko Kishimoto, Hiromi Takahashi-Iwanaga, Masahiko Watanabe M, and Toshihiko Iwanaga*

Laboratory of Histology and Cytology, Department of Anatomy, Hokkaido University Graduate School of Medicine, Sapporo 060-8638, Japan

* Corresponding author. Kita 15-Nishi-7, Kita-ku, Sapporo 060-8638, Japan

E-mail address: tiwanaga@med.hokudai.ac.jp

Abstract

The blood-brain barrier in the neonatal brain expresses the monocarboxylate transporter (MCT)-1 rather than the glucose transporter (GLUT)-1, due to the special energy supply during the suckling period. The hyaloid vascular system, consisting of the vasa hyaloidea propria and tunica vasculosa lentis, is a temporary vasculature present only during the early development of mammalian eyes and later regresses. Although the ocular vasculature manifests such a unique developmental process, no information is available concerning the expression of endothelial nutrient transporters in the developing eye. The present immunohistochemical study using whole mount preparations of murine eyes found that the hyaloid vascular system predominantly expressed GLUT1 in the endothelium, in contrast to the brain endothelium. Characteristically, the endothelium in peripheral regions of the neonatal hyaloid vessels displayed a mosaic pattern of MCT1-immunoreactive cells scattered within the GLUT1-expressing endothelium. The proper retinal vessels first developed by sprouting angiogenesis endowed with filopodia, which were absolutely free from the immunoreactivities of GLUT1 and MCT1. The remodeling retinal capillary networks and veins in the surface layer of the retina mainly expressed MCT1 until the weaning period. Immunostaining of MCT1 in the retina revealed fine radicular processes projecting from the endothelium, differing from the MCT1-immunonegative filopodia. These findings suggest that the expression of nutrient transporters in the ocular blood vessels is differentially regulated at a cellular level and that the neonatal eyes provide an interesting model for research on nutrient transporters in the endothelium.

Keywords: GLUT1, MCT1, hyaloid artery, retina, angiogenesis, immunohistochemistry

1. Introduction

Brain endothelial cells, an essential element of the blood-brain barrier, express the glucose transporter (GLUT)-1 to uptake glucose from the blood circulation. In particular, the endothelium in the neonatal brain expresses more intensely monocarboxylate transporter (MCT)-1 than GLUT1 in order to respond to the special energy supply since neonates largely depend on monocarboxylates such as ketone bodies and lactate derived from milk to serve as energy sources (Gerhart et al., 1997; Pellerin et al., 1998). Actually, the concentration of ketone bodies and lactate in the brain circulation is high in rodents during the suckling period but lowers after the weaning period (Vannuci and Simpson, 2003). MCT1, the first identified member of the MCT family (Garcia et al., 1995), comprises membrane-bound channels that transport lactate, ketone bodies, and other monocarboxylates—along with protons (pH), down their concentration gradients (for review, Halestrap and Meredith, 2004; Halestrap, 2012, 2013). In adults, all of the blood-tissue barriers maintain the expression of both MCT1 and GLUT1, as represented by the retinal pigment epithelium and brain vascular endothelium (Iwanaga and Kishimoto, 2015).

The ocular vascular system in developmental stages is characterized by the existence of the hyaloid vascular system, which regresses during the later developmental stages of the eyes. The hyaloid artery, a branch of the opthalamic artery, enters inside the fetal eyes through the optic disc, branches off, and runs toward the lens via two routes. A bundle of blood vessels that continues in a straight course from the hyaloid artery reaches the posterior pole of the lens to form the tunica vasculosa lentis (TVL) (Cairns, 1959; Hida, 1982). The vessels of TVL radiate spokewise and wholly cover the posterior surface of the lens. Another group of vessels branching at the proximal position extends in the vitreous along the internal

surface of the retina to yield the vasa hyaloidea propria (VHP). The VHP nourish the avascular inner retina and produce the primary vitreous, but their regress is earlier than other hyaloid vascular systems (Jack, 1972; Hida, 1982; Ito and Yoshioka, 1999), the regression process coinciding with the development of the proper retinal vessels (Cairns, 1959; Ashton 1968). Some branches of VHP anastomose with the TVL at the equator of the lens.

In the later stages of ocular development, the central retinal artery radiates into six arterial branches to construct a permanent vascular system for directly supplying the blood to the inner retina. Sprouting angiogenesis is predominant as the mode of development of the retinal vasculature, though some studies opt for vasculogenesis with the formation of blood islands (McLeod et al., 2012; also see Saint-Geniez and D'Amore 2004). The retinal vascular system provides a suitable sample for studies of angiogenesis or vasculogenesis, due to the easy preparation of whole mount preparations for overviewing. The hyaloid vessels possess tight junctions between endothelial cells that limit diffusion into the perivascular space (Braekevelt and Hollenberg, 1970; Townes-Anderson and Raviola, 1982), suggesting a need for transporters specific for each nutrient, like the blood-brain barrier. However, no information is available regarding the expression of MCTs and GLUTs in the angiogenesis of ocular tissues, and the question arises as to when predominant nutrient transporters switch during development. Studies on the retinal angiogenesis have focused on specific angiogenic molecules such as platelet-derived growth factor (PDGF) (Fruttiger et al., 1996) and vascular endothelial growth factor (VEGF) (Gerhardt et al., 2003), guidance by neuronal/glial elements (Fruttiger et al., 1996; Zhang et al., 1997), adhesion molecules including R-cadherin (Dorrell et al., 2002), and chemokines (Strasser et al., 2010).

Our preliminary study confirmed the predominant expression of MCT1 with a less intense expression of GLUT1 in the endothelium of blood capillaries in the neonatal brain, in agreement with previous studies, while we found a different expression pattern of MCT1 and GLUT1 in the eyes of neonatal mice. We further recognized the development of unique radicular projections from the MCT1-expressing endothelium in the retina. Here we report the morphological characteristics of GLUT1/MCT1-expressing vessels in the eye during the developmental stage of mice to characterize the ocular angiogenesis differentially expressing MCT1 and GLUT1.

2. Methods

2.1. Animals and tissue sampling

Pregnant ddY mice were supplied by Japan SLC (Shizuoka, Japan). The eyeballs of E16.5 and E18.5 embryos, neonates of postnatal day 0–3, 5, 7, 9, 11, 13, 15, 20, 25, and adult mice were used in the present study. Mice were sacrificed by the intraperitoneal injection of an overdose of pentobarbital sodium (Schering Plough Animal Health, the Netherlands). The eyeballs were enucleated and fixed for 2–6 h in 4% paraformaldehyde dissolved in 0.1 M phosphate buffer, pH 7.4. The retina and lens were isolated from eyeballs under a dissecting microscope. Some of the fixed tissues were dipped in 30% sucrose solution overnight at 4^{o}C, embedded in O.C.T. compound (Sakura Finetek, Tokyo, Japan), and quickly frozen in liquid nitrogen. Frozen sections of 12 μm in thickness were mounted on poly-L-lysine-coated glass slides.

All experiments using animals were performed under protocols following the Guidelines for Animal Experimentation, Hokkaido University Graduate School of Medicine.

2.2. Immunohistochemistry

After immersion in 0.01 M phosphate buffered saline (PBS) containing 0.3% Triton-X100, the whole mount preparations and sections were pre-incubated with a normal donkey serum. For double immunofluorescence, they were incubated overnight (for sections) or 4 days (for whole mount preparations) with a mixture containing two of a rabbit anti-mouse MCT1 antibody (469–493 amino acids of mouse MCT1; Kaji et al., 2015), guinea pig anti-GLUT1 antibody (460–492 amino acids of mouse GLUT1; Sakai et al., 2003), and rat anti-mouse CD31 antibody (MEC 13.3, 1:900: BD Pharmingen, Tokyo, Japan). The antibodies for MCT1 and GLUT1 were originally produced by an author of this study (M.W.) and characterization of the MCT1 antibody including immunoblotting analysis was described in our previous study (Kaji et al., 2015). The sites of antigen-antibody reactions were detected by using Cy3-labeled anti-rat or guinea pig IgG (1: 400 in dilution; Jackson ImmunoResearch, West Grove, PA) and AlexaFluor 488-labeled anti-rabbit IgG (1: 200 in dilution; Invitrogen, Carlsbad, CA). Some of the immunostained sections were counterstained with SyTO 13 (SYTOX, Invitrogen) for observation of the nuclei. Stained samples were mounted with glycerin-PBS and observed under a confocal laser scanning microscope (Fluoview; Olympus, Tokyo, Japan). The specificity of immunoreactions on sections was confirmed according to a conventional procedure, including absorption tests. Immunoreactivities with MCT1 and GLUT1 antibodies were completely abolished using the primary antibodies preabsorbed with corresponding antigens (mouse MCT1 and GLUT1).

2.3. Silver-intensified immunogold method for electron microscopy

Frozen sections, 10–14 μm in thickness, were pretreated with normal donkey serum for 30 min, incubated with the rabbit anti-MCT 1 antibody (1 μg/mL) overnight, and subsequently reacted with goat anti-rabbit IgG covalently linked with 1-nm gold particles (1:200 in dilution; Nanoprobes, Yaphank, NY). Following silver enhancement using a kit (HQ silver; Nanoprobes), the sections were osmicated, dehydrated, and directly embedded in Epon. Ultrathin sections were prepared and stained with an aqueous solution of uranyl acetate and lead citrate for observation under an electron microscope (H-7100; Hitachi, Tokyo, Japan).

2.4. Scanning electron microscopy (SEM)

Under pentobarbital anesthesia, mice at postnatal day 7 were transcardially perfused with Lock's solution saturated with O_2 and subsequently with a mixture containing 2.5% glutaraldehyde and 1.0% paraformaldehyde in 0.1 M phosphate buffer, pH 7.4. Posterior halves of the eyeballs and portions of the cerebral cortex were removed, cut into fine pieces, about 1.5 mm in size, and immersed in the same fixative overnight. The fixed tissue pieces were macerated with 6N NaOH for about 18 min at 60 ^{o}C (Takahashi-Iwanaga and Fujita T, 1986), rinsed and mildly disrupted by suction and ejection with a glass pipette in 0.02 M phosphate buffer (pH 7.3). After disruption the specimens were immersed in 1% tannic acid buffered with 0.1 M phosphate (pH 7.3), followed by 1% OsO_4 buffered with phosphate (0.1 M, pH 7.2) for 1 h. The osmicated specimens were dehydrated through a graded series of ethanol, transferred to isoamyl acetate, and critical-point-dried with liquid CO_2. The dried specimens were coated with osmium in a plasma osmium coater (Nippon Laser and Electronics Laboratory, Nagoya, Japan), and examined in a Hitachi SU8010 scanning electron microscope (Hitachi, Tokyo, Japan) at an acceleration voltage of 5 kV.

3. Results

3.1. Hyaloid vascular system

The hyaloid vascular system that is unique to developing eyes gives rise to two types of vascular networks running in the vitreous: the vasa hyaloidea propria (VHP) and the tunica vasculosa lentis (TVL). Immunostaining using the antibody against CD31, a marker of vascular endothelium, in whole mount preparations of neonatal eyes revealed that the VHP were a broad vascular reticulum spreading in the vitreous (Fig. 1a), and that, after sending out VHP, the hyaloid artery formed a tuft of branches to run straight in the center of the vitreous toward the lens (TVL in Fig. 1b). Concomitantly with the regression of these vessels in postnatal stages, sprouting angiogenesis yields blood vessels extending in the surface layer of the retina to construct a proper and permanent vascular system (red-colored vessels in Fig. 1b). These images well correspond with SEM and stereomicroscopic observations including plastic casting and dye-injected samples in previous studies using rodents (Cairns, 1959; Hollenberg and Dickson, 1971; Hida, 1982; Ito and Yoshioka, 1998).

The endothelium of VHP and TVL in fetuses (E16.5 and E18.5) and neonates in this study was essentially immunoreactive for GLUT1 (Fig. 1b, c). Observation of tissue sections from neonates at day 3 showed that GLUT1/CD31-double positive vessels of the VHP and TVL were distributed on the surface of the retina and lens, respectively (Fig. 2). The proximal portions of VHP took a comparatively straight course, while the distal portions pursued an undulating course and frequently branched and anastomosed (Figs. 1c, 3a). The blood vessels of VHP were at least twice—or more—thicker than the retinal capillaries. Although the VHP were immunolabeled for GLUT1 along their entire length, a small number of MCT1-expressing cells

intermingled with the GLUT1/CD31-positive endothelium in neonates (Fig. 3). The appearance of the MCT1-expressing cells was higher in frequency at the periphery of VHP. The endothelial cells in these regions differentially expressed either GLUT1 or MCT1, showing complementary expressions with a mosaic pattern (Supporting Figure 1a, b).

The blood vessels of TVL were also essentially immunoreactive for GLUT1 (Fig. 4a, b). In a view of the posterior surface of the lens, the TVL displayed a dense network which completely matched the vascular network visualized with the CD31 antibody (Fig. 4a, b). Again a minor population of MCT1-expressing cells was dispersed in the GLUT1/CD31-expressing endothelium at the posterior (Fig. 5) and lateral surfaces (equator face) of the lens (Fig. 6). The TVL vessels ran anteriorly, partially covering the anterior face of the lens, where they acquired a palisade-like array (arrows in Fig. 7) (corresponding to a row of straight capsulo-pupillary vessels noted by Hollenberg and Dickson, 1971). Some of them anastomosed with vessels of the pupillary membrane, a vascular network covering the anterior surface of the lens (PM in Fig. 7). Blood vessels in the pupillary membrane, which start regressing after birth, were small in diameter and often fragmentary at days 2–9, but still expressed GLUT1 rather than MCT1. Thus, the hyaloid vascular system expressed GLUT1 in its entire length, in contrast to the retina and brain endothelia with their predominant expression of MCT1, as mentioned below.

3.2. Vascular systems in the developing retina

In mice, vascularization of the retina begins around the optic disc at birth, and then typical sprouting angiogenesis expands peripherally. Until day 3, growing capillaries labeled with the antibody against CD31 were absolutely free from the

immunoreactivites for MCT1 and GLUT1 (Fig. 1b). A small nest of MCT1-immunoreactive capillaries appeared in the retina around the optic disc by postnatal day 5 and extended in the superficial layer of neonatal retina until day 7 (Fig. 8). Double immunostaining with MCT1 and CD31 demonstrated more clearly whole images of the angiogenesis with respect to the region-specific transporter expression (Fig. 9). The central retinal artery and its radial branches—usually six branches—lacked the expression of either GLUT1 or MCT1 in the endothelium. They were therefore hard to be visualized in preparations stained for GLUT1 and MCT1 (Fig. 8). In contrast, veins as well as blood capillaries predominantly expressed MCT1 (Fig. 8). The capillary plexus was very dense around veins but scanty near arteries, forming a periarterial capillary-free zone (Fig. 9). A double staining with MCT1 and CD31 highlighted a migrating vascular front endowed with filopodia at the growing tips (Figs. 9, 10). This sprouting area visualized by the CD31 antibody never expressed MCT1 or GLUT1. The sprouting, which started at the optic disc at day 0, reached the periphery of retina (ora serata) by day 9. The immature capillary plexus then changed to a mature capillary plexus, which is incorporated in the hierarchically organized artery-capillary-vein construct. The mature capillary plexus formed a vascular meshwork with uniform morphology and was not endowed with any typical filopodia seen at the sprouting area. The sprouting area and mature capillary plexus respectively correspond to the angiogenic front and the central plexus in the developing retina noted by Pitulescu et al. (2010). The central plexus may be equivalent to the remodeling plexus (Gerhardt et al., 2003). Desmin, a major component of muscle-specific intermediate filaments, was expressed in vascular smooth muscle cells and pericytes during angiogenesis. Growing capillaries are covered by desmin-immunoreactive pericytes at earlier angiogenetic processes (Adams and Alitalo, 2007). In the growing

retina, pericytes enveloped both the MCT1-expressing central plexus and CD31-labeled angiogenic front (Supporting Figure 2).

The immunoreactitivty for GLUT1 in the remodeling capillaries gradually increased in intensity after day 11 and were comparable in intensity with MCT1 immunoreactivity at day 20. At day 25, GLUT1 immunoreactivity in the capillaries and veins was more intense than MCT1 immunoreactivity.

3.3. Radicular projections in MCT1-expressing endothelia

At high magnification, the MCT1-positive capillaries that course immediately beneath the inner surface of the day 7 retina displayed numerous fine, long projections (Fig. 11). The projections displayed a consistent thickness—smaller than 0.5 μm in diameter—and did not branch dendritically, in contrast to filopodia which were thicker than 5 μm at proximal region and irregular in shape with tapered tips. The radicular projections were not associated with desmin-expressing pericytes. These projections occurred solitarily or in small groups along the entire length of the capillaries and spread over the surrounding retinal tissue at a generally constant density. In this sense, the fine endothelial projections, here designated as radicular projections, resemble the absorptive hairs of plant radicles rather than the filopodia that usually fan out from single foci of sprouting tip cells at the angiogenic front. The radicular projections were not associated with desmin-expressing pericytes (Supporting Figure 2b). MCT1-expressing veins possessed similar projections, but MCT1-immunonegative arteries were not provided with them (Fig. 11a). The radicular projections peaked in number and density at the mid-stage of suckling (postnatal days 5–11). They decreased in number at day 15 and almost disappeared by day 20. Similar MCT1-labeled projections were found in the capillaries of the neonatal brain at the

same stages (Supporting Figures 1c, d, and 3).

After the hydrolytic removal of the vitreous combined with mechanical disruption of the Müller cell and astrocyte processes, capillary networks in the inner layer of the day 7 retina were exposed under SEM (Fig. 12). The radicular projections were dispersed along the entire extent of the basal surfaces of the capillary endothelia, consistent with the immunohistochemical observations. The endothelial radicles ranged in thickness between 0.2–0.5 μm and occasionally displayed swellings and branchings along their courses. The great majority of the fine projections originated from boundaries of the endothelial cells, while the remainder occurred in central regions of the cell bases.

4. Discussion

The present immunohistochemical study using the eyes of neonatal mice revealed a predominant expression of GLUT1 in the endothelium of the hyaloid vascular system, which is programmed to regress coincidentally with the development of the proper retinal vessels. The retinal angiogenesis displayed stage- and region-specific expressions of MCT1 and GLUT1 in the endothelium: the angiogenic front expressed neither GLUT1 nor MCT1, while matured capillaries and veins of the central plexus expressed MCT1. Another characteristic figure of the retinal MCT1-expressing endothelium in neonates was the existence of long radicular projections different from filopodia routinely seen in the sprouting angiogenesis. The predominant nutrient transporters in the retinal vessels changed from MCT1 to GLUT1 after weaning, as observed in the brain.

4.1. Hyaloid vascular system expresses GLUT1

The VHP derived from the hyaloid artery ramify into many branches which anastomose with each other to form a vascular network throughout the vitreous. The hyaloid artery also produces the TVL, consisting of a dense vascular network covering the posterior and lateral faces of the lens. The VHP and TVL in mice have been reported to start regressing after postnatal day 6 (Ito and Yoshioka 1999), mainly due to the apoptosis of endothelial cells (Mitchell et al., 1998; Taniguchi et al., 1999). The present immunohistochemistry revealed that the endothelium of VHP and TVL in neonatal mice essentially expressed GLUT1, in sharp contrast to retinal capillaries and veins expressing MCT1. This unique expression of GLUT1 in the hyaloid vascular system may be attributable to its being a transitory vasculature or a special vascular type. Although the VHP and TVL manifest capillary-like arborizations, a study based on SEM observation has considered that the TVL lacks true capillaries and retains its arterial character until attaining the lateral, palisade-like vasculature (Strek et al., 1993). This idea is supported by the fact that arborized vessels of the VHP and TVL have a much larger diameter than typical capillaries in the retinal surface (Hida, 1982; Strek et al., 1993), as confirmed by the present study. Also, Saint-Geniez and D'Amore (2004) have considered that all hyaloid vessels are arterial in type. However, since other researchers have described the TVL as capillaries in the mouse (Mitchell et al., 1998) and rat (Braekevelt and Hollenberg, 1970) or "mostly capillaries or pericytic venules" in the rat (Latker and Kuwabara, 1981), the identification of vascular types in the TVL and VHP requires further analysis using marker substances.

Interestingly, dispersed MCT1-expressing endothelial cells intermingled with GLUT1-expressing endothelial cells, especially at the periphery of the hyaloid vessels. Although the significance of the mosaic expression pattern of GLUT1/MCT1 is unknown, this indicates a precise regulation of the GLUT1 and MCT1 expression at a

cellular level during the ocular angiogenesis; such an expression pattern was not observed in the endothelium of developing brain.

4.2. Differential expression of MCT1 and GLUT1 in the retinal vasculogenesis

The hyaloid vasculature starts to regress gradually after birth, while it gives rise to a superficial vascular plexus in the retina. During the first 10 days after birth in mice, a neovasculature extends from the optic disk toward the periphery within the nerve fiber layer of the retina and then constructs deep vascular networks reaching into the inner retina (Dorrell et al., 2002; Gerhardt et al., 2003). The retina is suitable for the study of normal and pathological angiogenesis, due to the easy use of whole mount preparations (Pitulescu et al., 2010). Moreover, we can extrapolate obtained findings to the brain angiogenesis (Gariano and Gardner, 2005).

Some studies using neonatal rodents have documented the predominant expression of MCT1 with the less intense expression of GLUT1 in the endothelium of capillaries in the retina (Bergersen et al., 1999: Chidlow et al., 2005), as demonstrated in the brain (Gerhart et al., 1997; Pepperin et al., 1998; Vannucci and Simpson, 2003). The present study confirmed the predominant expression of MCT1 in veins as well as capillaries of the neonatal retina by use of the whole mount preparations. The intense expression of MCT1 in the developing retina may respond to the uptake of monocarboxylates deriving from milk and circulating in the blood, as indicated in the brain (Vannucci and Simpson, 2003). The predominant expression of MCT1 in the central plexus is equivalent to vessels in the parenchyma of brain, which are largely capillaries in type. The shift from MCT1 to GLUT1 expression also occurred after weaning in the developing retinal vasculature. However, no information has been available for stage-dependent and regional expressions of MCT1/GLUT1 in the retinal angiogenesis.

The present staining was able to distinguish the angiogenic front from the central plexus, based on the expression of MCT1 and GLUT1: the angiogenic front never expressed GLUT1 or MCT1, while the central plexus or remodeling plexus expressed MCT1. Retinal arteries were free from any expression of GLUT1 and MCT1 during angiogenesis.

4.3. Formation of radicular projections in MCT1-expressing endothelia of the retina and brain

During retinal angiogenesis, the sprouting tips of blood vessels are always endowed with filopodial extensions (Dorrell et al., 2002; Gerhardt et al., 2003; Strasser et al., 2010). One surprising feature observed in the present study was the long radicular projections from capillaries of the central plexus, as clearly shown by the immunostaining of MCT1 and SEM observation. We were able to observe the same structures in the brain of murine neonates by both immunohistochemistry for MCT1 and SEM analysis (Supporting Figures 1c, d and 3). In addition to the morphology, these radicular projections of MCT1-expressing endothelial cells differ from the tip cell filopodia in the sprouting angiogenesis, which did not express MCT1. When the superficial vascular plexus reaches the peripheral region of the retina, vascular branches migrate from the inner plexus toward the outer retina between day 7 and day 9 in mice (Dorrell et al., 2002; Gerhardt et al., 2003). The penetrating vessels from the superficial plexus give rise to the deep vascular plexus, resulting in the adult type vascular construction around day 15 or 16 in the case of the rat retina (Cairns, 1959; Ashton, 1968). The MCT1-expressing radicular projections remarkably decreased in number 15 days after birth. This may indicate a novel feature of growing vessels shared by the brain endothelium, and could possibly be related to the special energy

demand in the suckling period. Migrating endothelial cells are known to be associated with underlying astrocytes during retinal angiogenesis (Holash and Stewart, 1993; Dorrell et al., 2002; Gerhardt et al., 2003). Although there is a possibility that the underlying astrocytes locally supply lactate produced by active glycolysis, the retinal vascular plexus initially formed on the astrocyte template subsequently dissociate from each other (Gerhardt et al., 2003). To reveal the involvement of MCT1 and monocarboxylates in the ocular angiogenesis, we are planning in vivo experiments using inhibitors and antibodies against MCT1.

In conclusion, the present study revealed concomitant but differential expressions of GLUT1 and MCT1 in the vascular system during ocular development. Some of these can be extrapolated to the brain vasculature; others are unique to the retinal vasculature. The radicular projections common to ocular and brain vasculatures may display a novel feature of angiogenesis different from the filopodial extensions.

Declaration of interest

The authors have no competing interests to declare.

References

Adams, R.H., Alitalo, K. 2007 Melecular regulation of angiogenesis and lymphangiogenesis. Nat. Rev. Mol. Cell Biol. 8, 464-478.

Ashton, N., 1968. Sone aspects of the comparative pathology of oxygen toxicity in the retina. Brit. J. Ophthal. 52, 505-531.

Bergersen, L., Jóhannsson, E., Veruki, M.L., Nagelhus, E.A., Halestrap, A., Sejersted, O.M., Ottersen, O.P., 1999. Cellular and subcellular expression of monocarboxylate transportes in the pigment epithelium and retina of the rat. Neuroscience 90, 319-331.

Braekevelt, C.R., Hollenberg, M.J., 1970. Comparative electron microscopic study of development of hyaloid and retinal capillaries in albino rats. Am. J. Ophthalmol. 69, 1032-1046.

Cairns, J. E., 1959. Normal development of the hyaloid and retinal vessels in the rat. Brit J Ophthal 43:385-393

Chidlow, G., Wood, J. P. M., Graham, M., Osborne. N. N., 2005. Expression of monocarboxylate transporters in rat ocular tissues. Am. J. Physiol. Cell. Physiol. 288, C416-C428.

Dorrell, M. I., Aguilar, E., Friedlander, M., 2002. Retinal vascular development is mediated by endothelial filopodia, a preexisting astrocyte template and specific R-cadherin adhesion. Invest. Opthalmol. Vis. Sci. 43, 3500-3510.

Fruttiger, M., Calver, A. R., Krüger, W. H., Mudhar, H. S., Michalovich, D., Takakura, N., Nishikawa, S., Richardson, W. D., 1996. PDGF mediates a neuron-astrocyte

interaction in the developing retina. Neuron 17, 1117-1131.

Garcia, C. K., Goldstein, J. L., Pathak, R. K., Anderson, R. G. W., Brown, M. S., 1994. Molecular characterization of a membrane transporter for lactate, pyruvate, and other monocarboxylates: implications for the Cori cycle. Cell 76, 865–873.

Gariano, R. F., Gardner, T. W., 2005. Retinal angiogenesis in development and disease. Nature 438, 960-966.

Gerhardt, H., Golding, M., Fruttiger, M., Ruhrberg, C., Lundkvist, A., Abramsson, A., Jeltsch, M., Mitchell, C., Alitalo, K., Shima, D., Betsholtz, C., 2003. VEGF guides angiogenic sprouting utilizing endothelial tip cell filopodia. J. Cell. Biol. 161, 1163-1177.

Gerhart, D. Z., Enerson, B. E., Zhdankina, O. Y., Leino, R. L., Drewes, L. R., 1997. Expression of monocarboxylate transporter MCT1 by brain endothelium and glia in adult and suckling rats. Am. J. Physiol. 273 (Endocrinol. Metab. 36), E207-E213.

Halestrap, A. P., 2012. The monocarboxylate transporter family—structure and functional characterization. IUBMB Life 64, 1-9.

Halestrap, A. P., 2013. Monocarboxylic acid transport. Compr Physiol 3, 1611-1643.

Halestrap, A. P., Meredith, D., 2004. The SLC16 gene family—from monocarboxylate transporters (MCTs) to aromatic amino acid transporters and beyond. Pflugers Arch. 447, 619-628.

Hida, T., 1982. Hyaloid vascular system of the rat: a study on its topography examined by plastic cast. J. Jpn. Ophthalmol. Soc. 86, 315-327 (Acta Soc Ophthalmol Jpn)

Hollenberg, M.J., Dickson, D. H., 1971. Scanning electron microscopy of the tunica vasculosa lentis of the rat. Can. J. Ophthalmol. 6, 301-310.

Holash, J. A., Stewart, P. A., 1993. The relationship of astrocyte-like cells to the vessels that contribute to the blood-ocular barriers. Brain Res. 629, 218-224.

Ito, M., Yoshioka, M., 1999. Regression of the hyaloid vessels and pupillary membrane of the mouse. Anat. Embryol. 200, 403-411.

Iwanaga, T., Kishimoto, A., 2015. Cellular distributions of monocarboxylate transporters. Biomed. Res. (Tokyo) 36, 279-301.

Jack, R. L., 1972. Ultrastructure of the hyaloid vascular system. Arch. Ophthal. 87, 555-567.

Kaji, I., Iwanaga, T., Watanabe, M., Guth, P. H., Engel, E., Kaunitz, J. D., Akiba, Y., 2015. SCFA transport in rat duodenum. Am. J. Physiol. Gastrointest. Liver Physiol. 308, G188-G197.

Latker, C. H., Kuwabara, T., 1981. Regression of the tunica vasculosa lentis in the postnatal rat. Invest. Ophthalmol. Vis. Sci. 21, 689-699.

McLeod, D. S., Hasegawa, T., Baba, T., Grebe, R., d'Auriac, I. G., Merges, C., Edwards, M., Lutty, G. A., 2012. From blood islands to blood vessels: morphologic observations and expression of key molecules during hyaloid vascular system development. Invest. Ophthalmol. Vis. Sci. 53, 7912-7927.

Mitchell, C. A., Risau, W., Drexler, H. C., 1998. Regression of vessels in the tunica vasculosa lentis is initiated by coordinated endothelial apoptosis: a role for vascular

endothelial growth factor as a survival factor for endothelium. Dev. Dyn. 213, 322-333.

Pellerin, L., Pellegri, G., Martin, J. L., Magistretti, P. J., 1998. Expression of monocarboxylate transporter mRNAs in mouse brain: Support for a distinct role of lactate as an energy substrate for the neonatal vs. adult brain. Proc. Natl. Acad. Sci. USA 95, 3990-3995.

Pitulescu, M. E., Schmidt, I., Benedito, R., Adams, R. H., 2010. Inducible gene targeting in the neonatal vasculature and analysis of retinal angiogenesis in mice. Nat. Protocols 5, 1518-1534.

Saint-Geniez, M., D'Amore, P. A., 2004. Development and pathology of the hyaloid, choroidal and retinal vasculature. Int. J. Dev. Biol. 48, 1045-1058.

Sakai, K., Shimizu, H., Koike, T., Furuya, S., Watanabe, M., 2003. Neutral amino acid transporter ASCT1 is preferentially expressed in L-Ser-synthetic/storing glial cells in the mouse with transient expression in developing capillaries. J. Neurosci. 23, 550-560.

Strasser, G. A., Kaminker, J. S., Tessier-Lavigne, M., 2010. Microarray analysis of retinal endothgelial tip cells identifies CXCR4 as a mediator of tip cell morphology and branching. Blood 115, 5102-5110.

Strek, W., Strek, P., Nowogrodzka-Zagórska, M., Litwin, J. A., Pitynski, K., Miodonski, A. J., 1993. Hyaloid vessels of the human fetal eye. A scanning electron microscopic study of corrosion casts. Arch. Ophthalmol. 111, 1573-1577.

Takahashi-Iwanaga, H., Fujita, T., 1986. Application of an NaOH maceration method to a scanning electron microscopic observation of Ito cells in the rat liver. Arch. Histol. Jpn.

49, 349-357.

Taniguchi, H., Kitaoka, T., Gong, H., Amemiya, T., 1999. Apoptosis of the hyaloid artery in the rat eye. Ann. Anat. 181, 555-560.

Townes-Anderson, E., Raviola, G., 1982. Morphology and permeability of blood vessels in the prenatal rhesus monkey eye: how plasma components diffuse into the intraocular fluids during development. Exp. Eye Res. 35, 203-230.

Vannuci, S. J., Simpson, I. A., 2003. Developmental switch in brain nutrient transporter expression in the rat. Am. J. Physiol. Endocrinol. Metab. 285, E1127-E1134.

Zhang, Y., Stone, J., 1997. Role of astrocytes in the control of developing retinal vessels. Invest. Opthalmol. Vis. Sci. 38, 1653-1666.

Figure legends

Fig. 1. A whole mount preparation of the retina immunostained for GLUT1 and CD31 at postnatal day 2. A coarse network of VHP is double-stained for GLUT1 and CD31 to appear yellow (**a**). A small nest of growing vasculature around the optic disc is stained red with the CD31 antibody only. An enlarged view of the center of the retina is shown in Fig. 1**b** and **c**. In this preparation, the proximal portion of the TVL displays a tuft of blood vessels. Note that TVL and VHP are immunoreactive for GLUT1 along their entire lengths. Bars 500 μm (a), 200 μm (b, c)

Fig. 2. Immunostaining of a tissue section from the eyeball of a day 3 neonate. The VHP and TVL are immunolabeled with both GLUT1 and CD31. Yellow colored vessels of VHP and TVL lie closely adjacent to the avascular retina and lens, respectively. An asterisk indicates a CD31-positive vascular sprouting in the surface layer of the retina. Bar 200 μm

Fig. 3. Double staining of MCT1 and CD31 in the VHP at postnatal day 3. MCT1-expressing endothelial cells, appearing yellow or green, are dispersed in the CD31-immunolabeled vessels of VHP. Fig. 3**b** is an enlarged view of Fig. 3**a**. Note that CD31-labeled vessels of VHP are very thick in diameter. Bars 200 μm (a), 100 μm (b)

Fig. 4. A posterior view of the lens showing the TVL immunostained for GLUT1 and CD31. Branched networks of TVL display a positive immunoreactivity for GLUT1 along their entire lengths. Bar 200 μm

Fig. 5. A higher magnification of a lens stained for MCT1 and CD31. Here again, some MCT1-expressing endothelial cells intervene in the CD31-positive vasculature on the posterior surface of the lens. Bar 100 μm

Fig. 6. An equatorial view of a lens stained for MCT1 and GLUT1. Some MCT1-expressing vessels intermingle with GLUT1-expressing vessels of the TVL. Bar 200 μm

Fig. 7. Anterior surface of the lens. The GLUT1-expressing vessels of the TVL run more parallel at the equator to show a palisade-like array (arrows). Some branches connect with thin vessels of the pupillary membrane (PM). Bar 200 μm

Fig. 8. An overview of retinal vessels visualized with MCT1 and GLUT1 antibodies. Six main branches of veins radiating from the optic disk and intervening capillary networks are immunoreactive for MCT1, but arteries (A) are negative in reaction. The tuft of TVL is labeled only with the GLUT1 antibody. Bar 200 μm

Fig. 9. The periphery of vasculature growing in the surface layer of retina shows two different parts, namely an angiogenic front (AF) and central plexus (CL). The former is immunoreactive for only CD31 and the latter is also positive for MCT1. Bar 200 μm

Fig. 10. A closer view of the sprouting tip provided with filopodia (arrows) visualized with the CD31 antibody. This corresponds to growing tips of immature capillary. Bar 50 μm

Fig. 11. The central plexus (CL) in the retina between a vein (V) and artery (A). The blood capillary and vein are immunoreactive for MCT1 (**a**). An enlarged view of capillaries (**b**, **c**) shows the existence of radicular projections. Bar 50 μm (a), 20 μm (b, c)

Fig. 12. Scanning electron micrographs of capillary vessels in the retina at neonatal 7 days. The extracellular matrix has been thoroughly removed by alkaline maceration to

expose the surface of endothelial cells. Many radicles project from the outer surface of endothelial cells (E). Bars 10 μm (a), 1 μm (b)

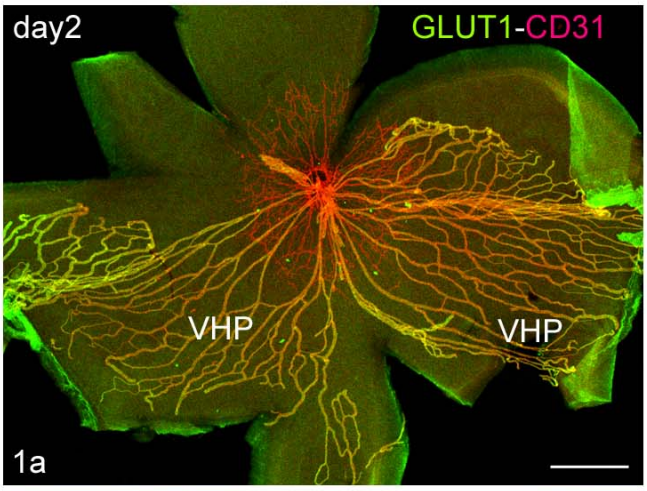
day2
GLUT1-CD31
VHP
VHP
1a

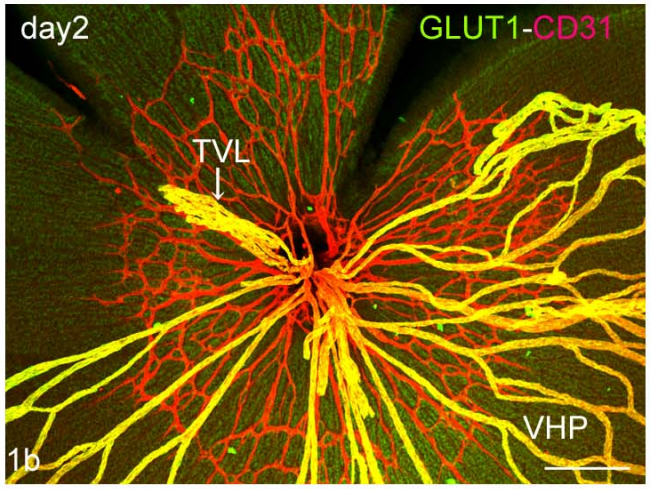
day2
GLUT1-CD31
TVL
VHP
1b

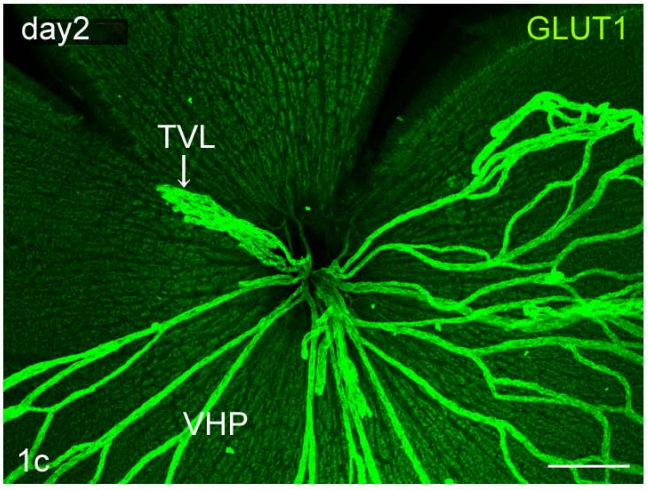
day2
GLUT1
TVL
VHP
1c

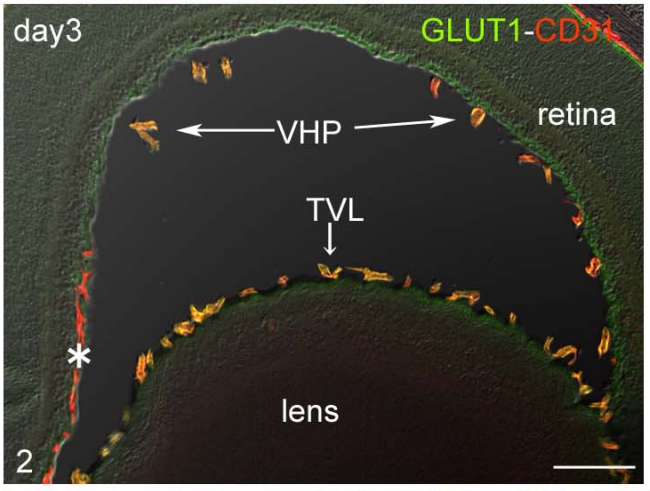
day3
GLUT1-CD31
VHP
retina
TVL
*
lens
2

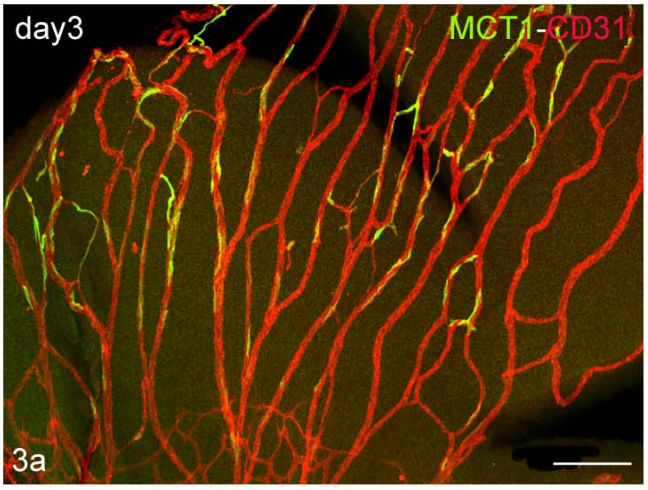
day3
MCT1-CD31
3a

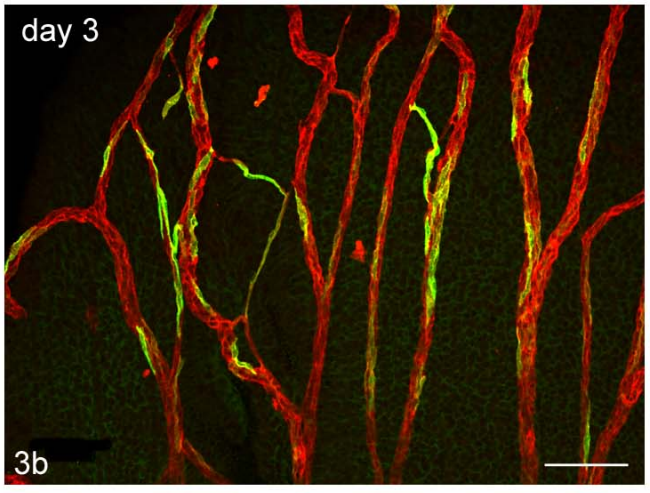
day 3
3b

Figures 1-3

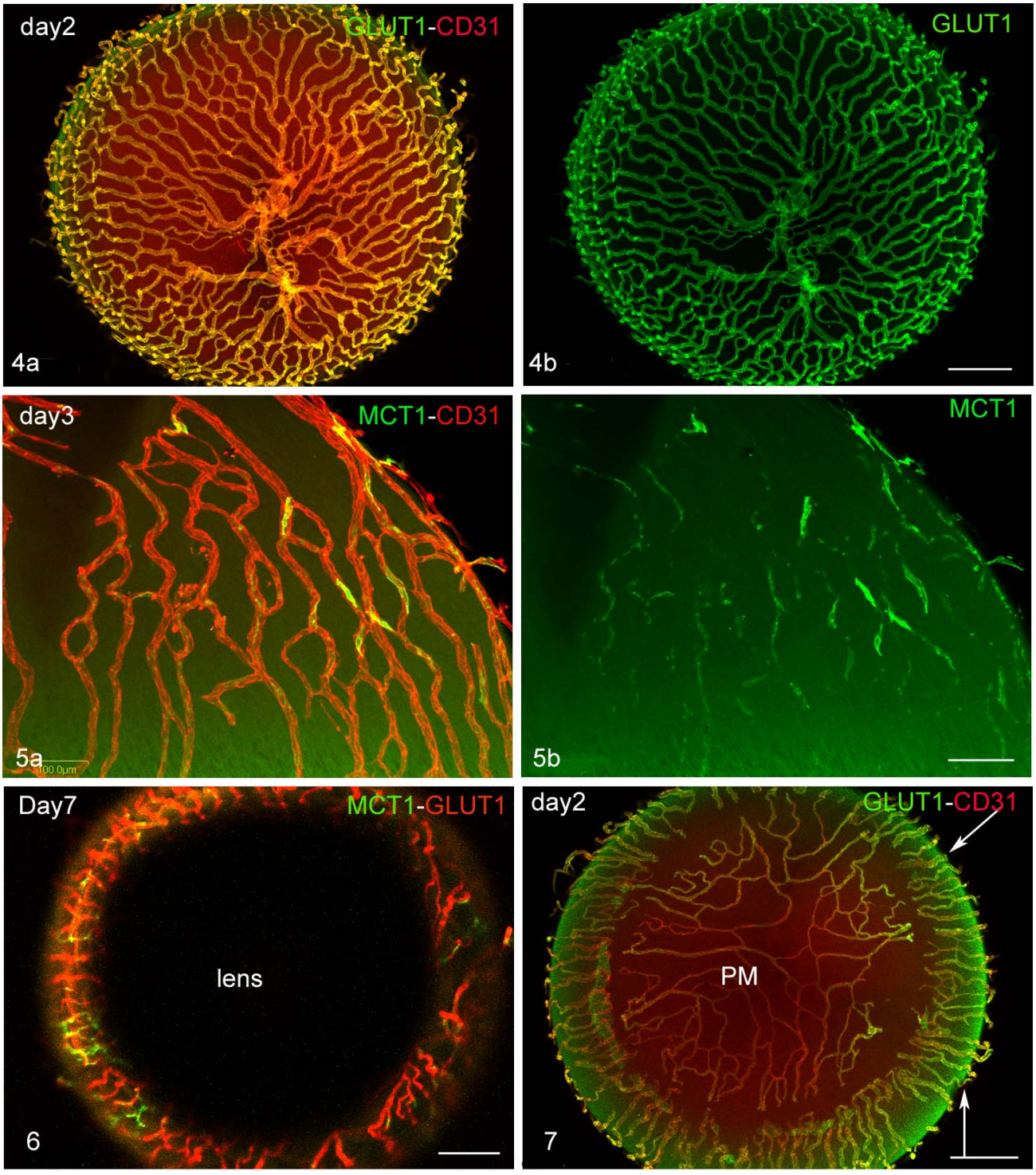
day2
GLUT1-CD31
4a
GLUT1
4b
day3
MCT1-CD31
5a
MCT1
5b
Day7
MCT1-GLUT1
lens
6
day2
GLUT1-CD31
PM
7

Figures 4-7

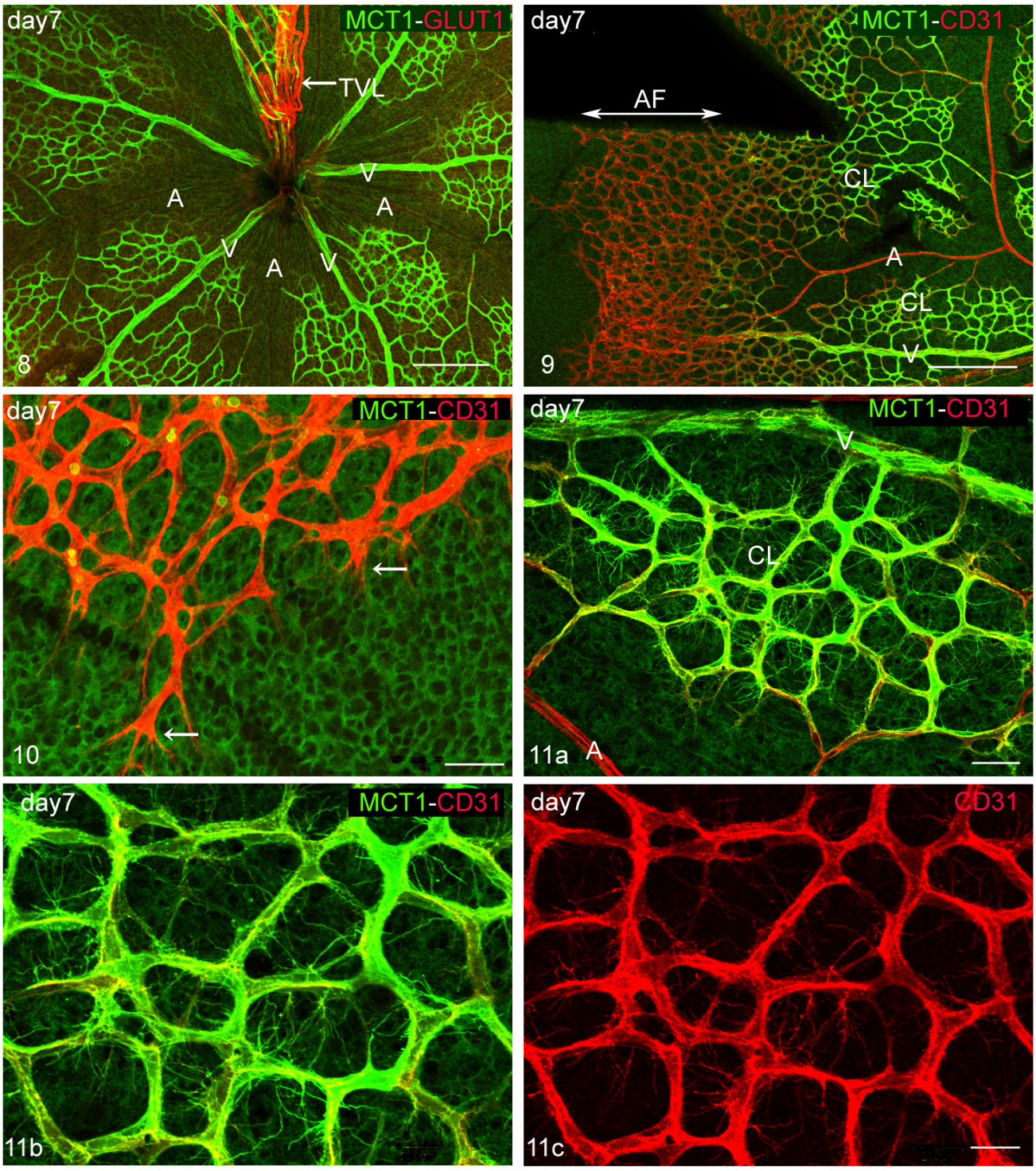
day7
MCT1-GLUT1
TVL
A
V
A
V
A
V
8
day7
MCT1-CD31
AF
CL
A
CL
V
9
day7
MCT1-CD31
10
day7
MCT1-CD31
V
CL
11a
A
day7
MCT1-CD31
11b
day7
CD31
11c

Figures 8-11

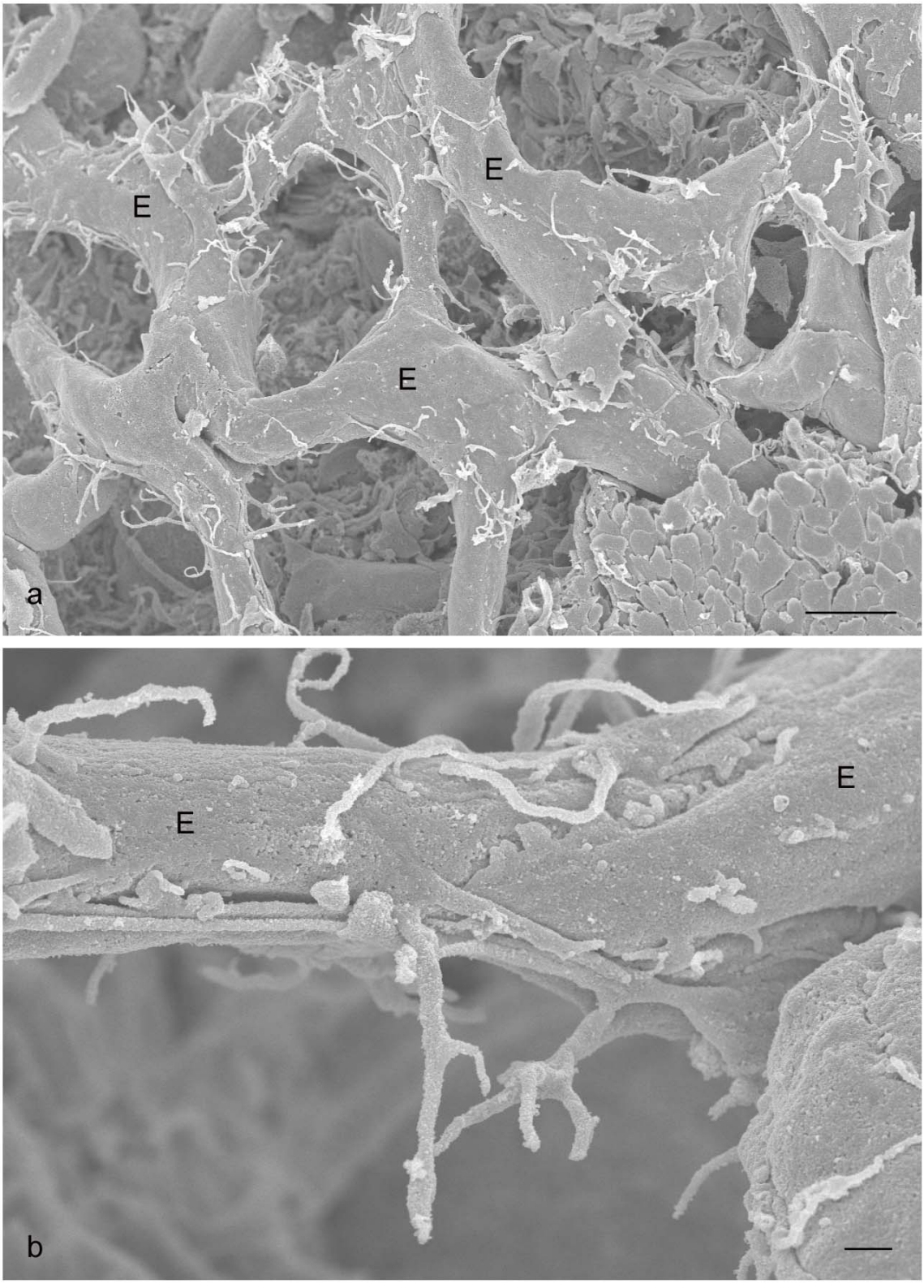

Figure 12